Electrical characteristics of soda lime silica glass at Pb, Pb/Cu and Bi/Cu anodes at high temperatures

J. K. HIGGINS AND F. V. ROUÉ

Lathom Laboratories, Pilkington Brothers, Ormskirk, Lancs., U.K.

The electrolysis of a soda-lime silica glass has been studied using Pb, Pb/Cu and Bi/Cu anodes at temperatures from 500 to 800°C. Generally, electrolyses at Pb/Cu anodes obeyed $1/I^2$ against t equations under these conditions whereas a $1/I$ against t relationship would be obtained for a Pb anode. At the Bi/Cu anode, containing a larger concentration of copper (9·9% as compared to 1·9%), the electrolysis current was almost constant for periods of seconds even at 600°C and less. With Pb anodes the temperature at which $1/I^2$ against t behaviour changed to $1/I$ against t increased as the temperature increased; it was 2·5 and 50 V at 600 and 700°C, respectively.

On the basis of these results and some pulse experiments which showed polarization at Pb but not at Pb/Cu anodes it is proposed that the behaviour at the latter, at least, can be explained by the electromigration of copper ions into the glass replacing the interstitial sodium ions and resulting in the formation of a surface layer of higher specific resistance than that of the bulk glass. A similar mechanism may occur at Pb anodes at higher temperatures.

1. Introduction

A recent series of experiments [1] suggested that the fast electrochemical changes occurring during the high temperature (600°C) electrolysis of soda lime silicate glasses at molten lead anodes involved the polarization of the glass near that electrode and the consequent setting up of a space charge region or electrical double layer there.

In order to extend the investigation, the experiments at the lead anodes were repeated at temperatures from 500 to 800°C and the effect of pulsing upon the polarization at the electrode was studied. In order to study the behaviour at liquid anodes, containing ions that could easily migrate into the glass, electrolyses were also carried out using molten anodes of Pb/Cu and Bi/Cu alloys.

2. Experimental

The experimental cell and furnace have been described in a previous paper [1]. The Pb/Cu and Bi/Cu alloys used were prepared by melting the analytical reagent metals in nitrogen/10% hydrogen for 1 h before casting. The copper concentrations in the two alloys were 1·9 and 9·9%, respectively.

At the higher temperature it was found that the molten alloys had sunk into the softened glass after removal of the electrolysis cell from the furnace. However, this did not alter the cross-sectional area for electrolysis and similar I/t plots were obtained for electrolyses performed at intervals of 5, 10, 20, 40 and 80 min after heating. During this time the molten metal anode had sunk progressively into the glass.
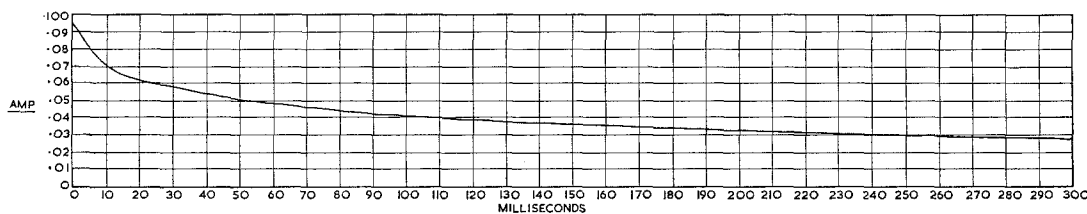
The electrical circuit was basically that des-

Fig. 1. Current time trace at 25 V. Pb/Cu anode at 600°C, speed 2 m s^{-1}.

cribed in reference [1]. However, the Measurement Research Control Unit was modified to supply a series of square wave pulses of variable mark space ratios from 10 ms to 100 s as well as the usual, single pulse. This was done using a basic 10 ms clock pulse and building up longer pulses as multiples of this using Fairchild MS1 logic chips; any number of pulses from 1 to 100 could be applied. The I/t traces were recorded using a UV Recorder, and the voltage decays on breaking the circuit with a Tektronix 564 storage oscilloscope.

3. Results

In Fig. 1 is shown an I against t trace for a Pb/Cu anode at 600°C at an applied voltage of 25 V. The current rises rapidly at first and then decays slowly to a lower value.

In Fig. 2 (a) and (b) are shown the $1/I^2$ against t and $1/I$ against t plots obtained under these conditions on successive pulsing at hourly intervals. Three effects contrast the behaviour at Pb anodes under the same conditions: (i) the equation obeyed for the first four electrolyses is of the form $1/I^2$ against t and not $1/I$ against t; (ii) the gradient remains substantially constant after successive pulses and the graphs are grouped together; (iii) even after repeated electrolyses when a $1/I$ against t relationship is eventually obeyed, the gradient remains constant on further pulsing.

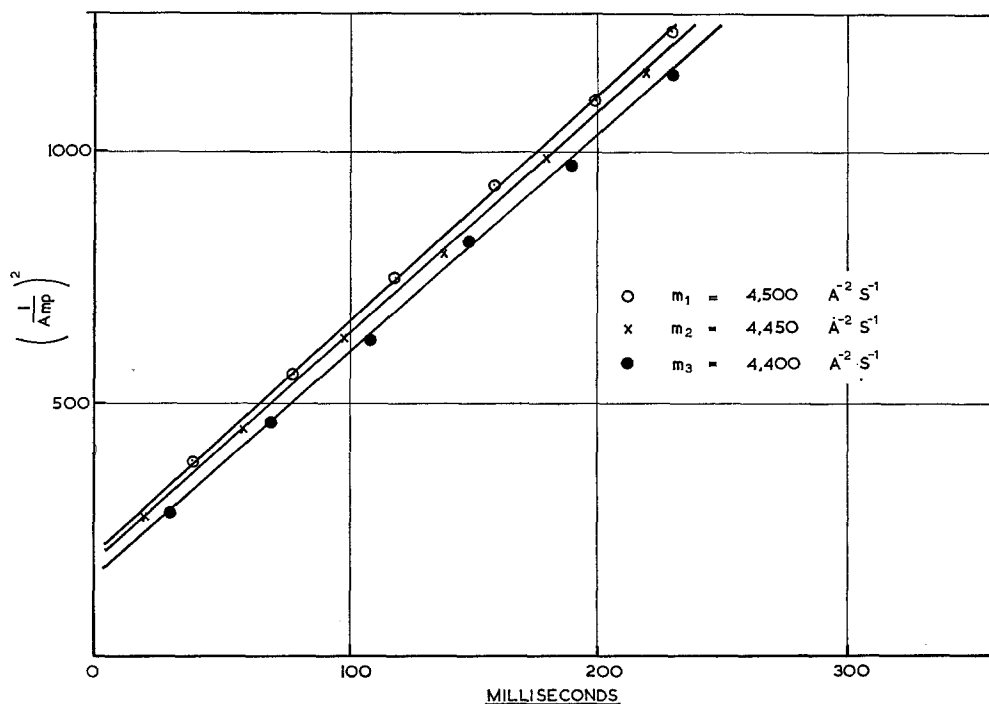It is furthermore clear from Table 1 that the $1/I^2$ against t type of behaviour persists for

Fig. 2. (a) Graph of (current reciprocal)^2 against time at 25 V. Pb/Cu anode at 600°C. Successive pulses.
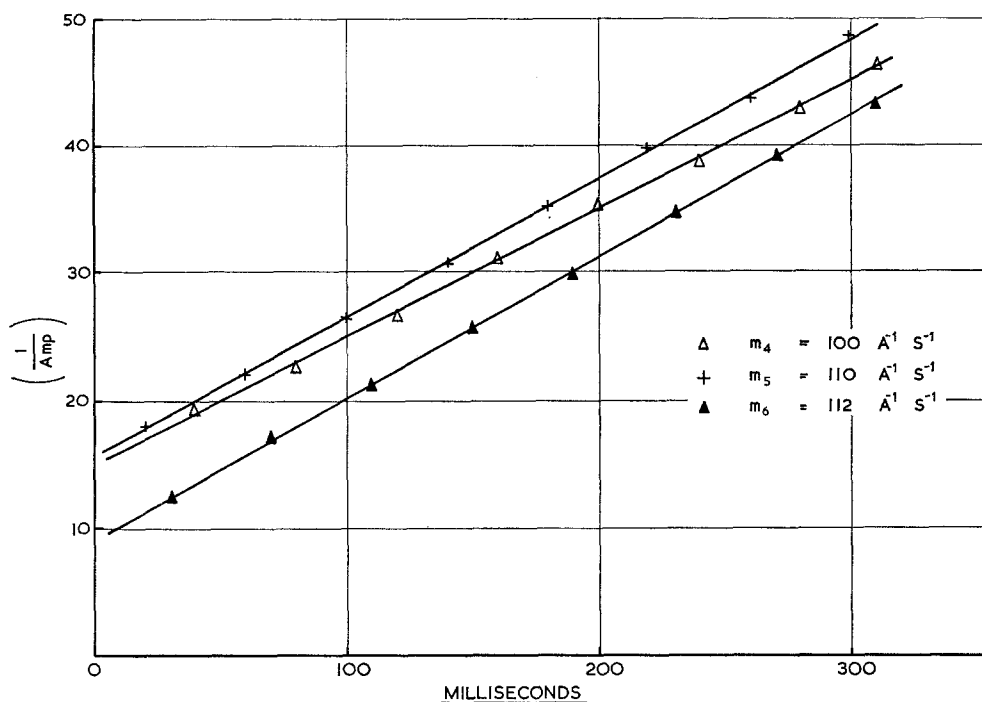
Fig. 2(b) Graph of current reciprocal against time at 25 V. Pb/Cu anode at 600°C. Successive pulses.

Table 1. *Variation of current–time equations at various temperatures using Pb/Cu and Pb anodes*

Temperature °C	Voltage (V)	m	a	Equation $(mt+a)I^2=1$	σ_x mhos cm^{-1} calc.	Range ms
			Pb/Cu Anodes			
600	25	4500	185	$(4500t+185)\, I^2 = 1$	$6\cdot8 \times 10^{-9}$	0–300
	50	300	35	$(300t+35)\, I^2 = 1$	$5\cdot0 \times 10^{-9}$	0–300
650	25	2450	25	$(2450t+25)\, I^2 = 1$	$1\cdot24 \times 10^{-8}$	0–350
700	25	212	1·6	$(212t+1\cdot6)\, I^2 = 1$	$1\cdot41 \times 10^{-7}$	0–300
800	25	—	—	$I\, 10^3 = -44t+785$	—	0–3000
			Pb Anodes			
500	25	433	4·6	$(433t+4\cdot6)\, I = 1$	—	0–350
600	25	190	7	$(190t+7)\, I = 1$	—	0–300
650	25	85	9	$(85t+4)\, I = 1$	—	0–400
700	12	13 000	100	$(13\,000t-100)\, I^2 = 1$	$2\cdot8 \times 10^{-8}$	0–300
	25	352	5	$(352t+20)\, I^2 = 1$	$8\cdot7 \times 10^{-8}$	0–300
750	25	205	7	$(205t+8)\, I^2 = 1$	$1\cdot48 \times 10^{-7}$	0–350
800	25	75	5	$(75t+9)\, I^2 = 1$	$4\cdot15 \times 10^{-7}$	0–300

Pb/Cu anodes up to 50 V at 600°C whereas for Pb anodes the $1/I^2$ against t relationship breaks down above 2·5 V [1]. At the higher temperature of 700°C, the $1/I^2$ against t relationship still holds but on raising the temperature to 800°C the current is almost constant with time during the electrolysis as is clear from Fig. 3. In the Bi/Cu system, with a considerably higher copper concentration the current remains constant at the lower temperature of 600°C, Fig. 4, and is
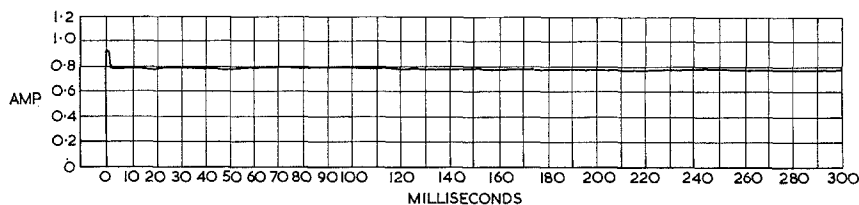
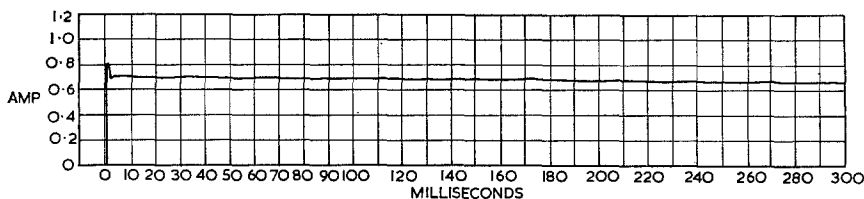Fig. 3. Current time trace at 25 V. Pb/Cu anode at 800°C, speed 2 m s^{-1}.

Fig. 4. Current time trace at 25 V. Bi/Cu anode at 600°C, speed 2 m s^{-1}.

of the same order as that for the Pb/Cu system at 800°C.

At the temperature previously studied using the Pb anode [1], the predominant behaviour observed was $1/I$ against t; equations of the type $1/I^2$ against t were only found when the applied voltage was 2·5 V or less. However, this alters when the temperature is raised. At 700°C, for example, $1/I^2$ against t relationships were found for voltages up to 50 V while at 800°C similar behaviour was observed until dielectric breakdown occurred at 27 V.

The fact that successive pulsing using Pb anodes gave displaced $1/I$ against t plots while it did not do so at Pb/Cu anodes suggests that there might be some form of polarization occurring in the former case [1] and not in the latter. In order to examine this question further both systems were submitted to a series of pulsed electrolyses in which the ON time was held constant at 20 ms and the OFF time increased progressively from 20 to 300 ms. The results at 600°C are shown in Figs. 5–7, where the

current I is plotted against the time and the time in milliseconds is plotted against the quantity of electricity supplied to the sample. It is clear for the Pb anodes (Fig. 6) that at any particular time the quantity of electricity supplied is greater the greater the OFF time, i.e. the greater the relaxation time between pulses.

Also, in the two cases the equations relating time to charge are different. At the Pb anode, log t is proportional to Σq while at the Pb/Cu anode t is proportional to Σq: the gradient of the log plot is approximately unity. This suggests that there is a different mechanism occurring in the two cases, the fact that t is proportional to Σq in the latter case suggesting that the electrolysis using a Pb/Cu anode resembles more a normal aqueous electrolysis than that using a Pb anode.

Finally, the voltage decay on removing the power supply was examined using the storage oscilloscope. The two photographs Fig. 8(a) and (b) at 600°C for Pb and Pb/Cu anodes show a slow decrease in the former case indicating
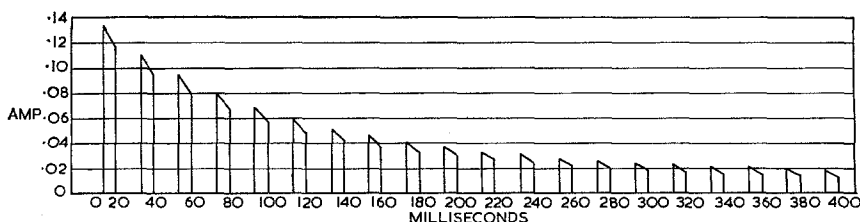

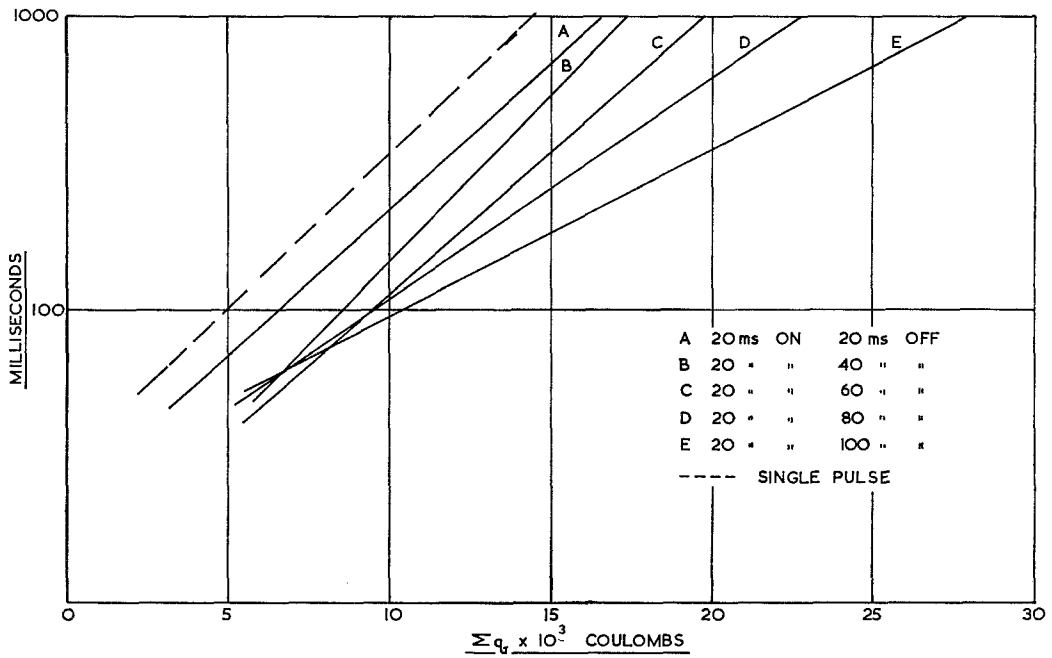Fig. 5. Current time trace at 25 V. Pb anode at 600°C, pulsed, speed 2 m s^{-1}.

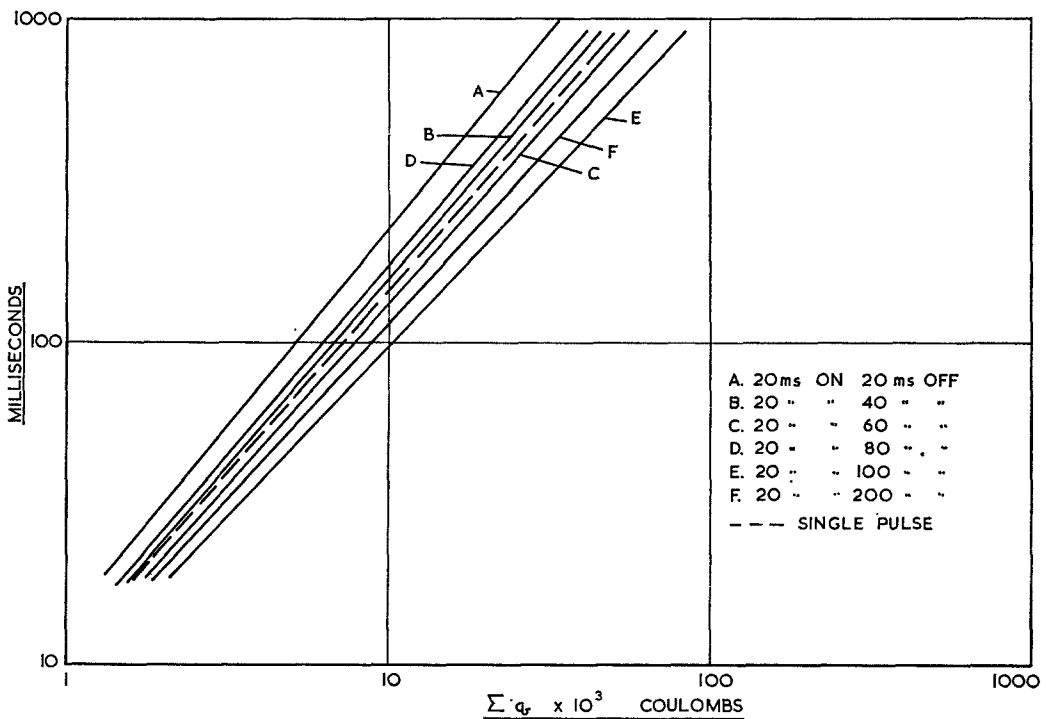Fig. 6. Graph of charge against time. Pb anode at 600°C, pulsed.

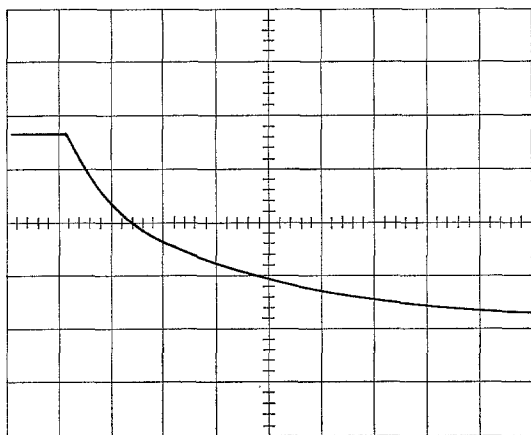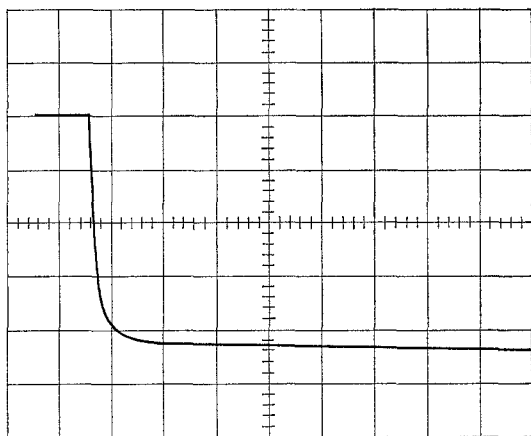Fig. 7. Graph of charge against time. Pb/Cu anode at 600°C, pulsed.

(a)

(b)

Fig. 8. Oscillogram of voltage decay against time at 600°C. Initial voltage 25 V, x-axis 2 ms cm^{-1}, y-axis 5 V cm^{-1}, (a) Pb anode, (b) Pb/Cu anode.

polarization and a rapid decrease in the latter case suggesting its absence.

In view of the two different relationships obtained at Pb and Pb/Cu anodes it is interesting to examine the behaviour under pulsing of the Pb anode at a higher temperature (800°C) where an $1/I^2$ against t type of relationship is obeyed. The results are given in Fig. 9 and it is seen that at this higher temperature all the graphs are now randomly grouped round the unpulsed graph, there is no progressive increase of charge with OFF time and a t against Σq equation is obeyed. These results suggest that raising the temperature eliminates the polarization.

4. Discussion

Most of the data obtained at the Pb/Cu anodes and at the Pb anodes at temperatures higher than 600°C obey the $1/I^2$ against t law. This can be derived by assuming that during electrolysis there is a layer formed near the anode of higher electrical resistance than that of the bulk glass, due to the replacement of mobile, interstitial sodium ions by copper or lead ions. The treatment, due to J. A. Yates, (see Appendix) is based on three assumptions:

(i) the current at any time can be expressed in terms of the specific conductivity (σ_x) of the treated layer:

$$I = \frac{\sigma_x V_x}{y} \qquad (1)$$

where V_x is the voltage drop across the layer of thickness y.

(ii) the current may also be expressed in terms of the specific conductivity (σ_{Na}) of the base glass:

$$I = \sigma_{Na}\left(\frac{V - V_x}{l - y}\right) \approx \sigma_{Na}\left(\frac{V - V_x}{l}\right) \qquad (2)$$

since the sample thickness, l, is much greater than the layer thickness, y.

(iii) the rate of penetration of anode material is proportional to the current:

$$\frac{dy}{dt} = \frac{I}{Fc} \qquad (3)$$

where c is the concentration of replaceable ions in g Eq cm^{-3} and F is the Faraday. The terms y and V_x may be eliminated from these expressions resulting, finally, in the expression:

$$I = \left[\frac{\frac{1}{2}V\sigma . cF_x}{t + \frac{\sigma_x . Fc . l^2}{2\sigma_{Na}^2 V}}\right]^{\frac{1}{2}} \qquad (4)$$

(see Appendix I).
This expression predicts that $1/I^2$ should be proportional to t.
Rearranging Equation (4) we have:

$$\left[\frac{2t}{V\sigma_x Fc} + \frac{l^2}{\sigma_{Na}^2 V^2}\right]I^2 = 1 \qquad (5)$$
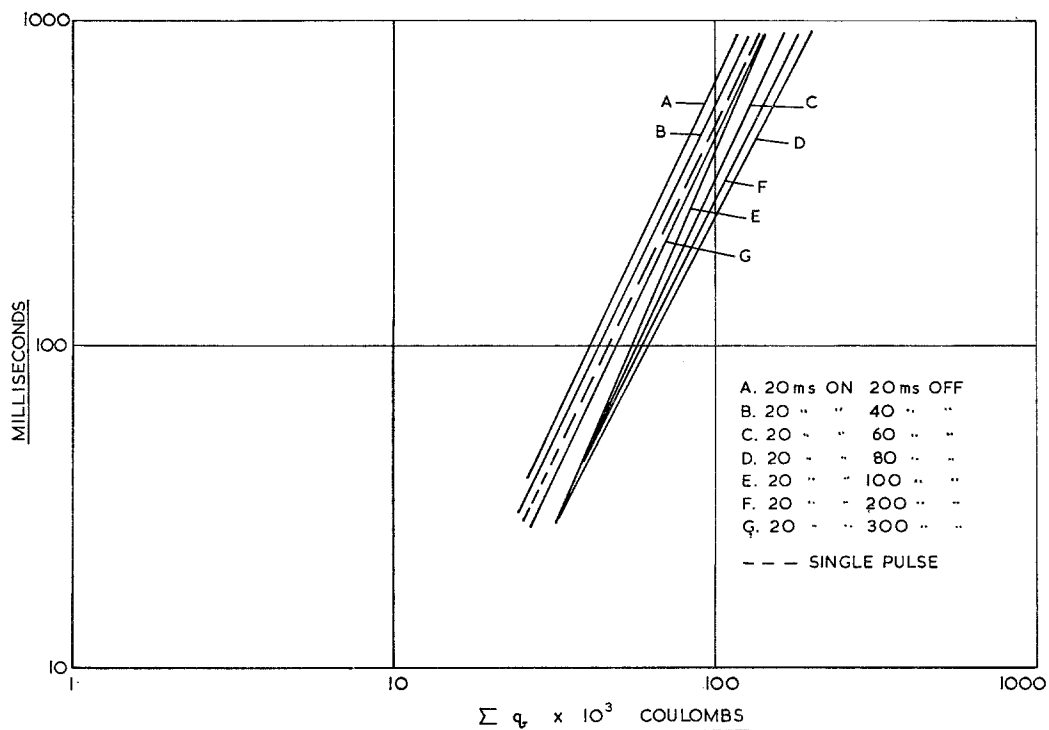
Fig. 9. Graph of charge against time. Pb anode at 800°C, pulsed.

This is of the same form as the equations involving I^2 in column 5 of Table 1 and, by comparing coefficients, values of σ_x at the different temperatures may be calculated. They are tabulated in column 6 of Table 1. There is, as expected, a steady increase of σ_x with temperature.

In addition, the thickness, y, of the high resistance surface layer may be calculated from the expression:

$$y = \frac{\sigma_x V_x}{I} \qquad (1)$$

if the values of σ_x, V_x and I are known. Inserting the value of I at 300 ms, at which point it is assumed that the full applied voltage is across the high resistance layer, values of y at the various temperatures have been calculated— (columns 5 and 6 of Table 2).

These calculated values of σ_x may be compared to the conductivities measured for fused silica by Owen and Douglas [2] and to those for lead silicate glass (PbO.SiO$_2$) measured by Strauss et al. [3]. Interpolated values of the specific conductivity of two samples of fused silica containing 4 and 0·04 p.p.m. of Na prepared by the electrical fusion of quartz crystals and the vapour phase decomposition of SiCl$_4$ are given in column 7 and column 8 of Table 2. Values of the specific conductivity of lead silicate glass (PbO.SiO$_2$) were measured by Strauss et al. in the range 200 to 400°C. Using the Rasch-Hinrichsen law these were extrapolated to the higher temperatures considered in this work and are given in column 9 of Table 2. It is clear that the values of σ_x are much closer to those of Owen and Douglas for I.R. electrically fused silica than to those of Strauss for lead silicate glass. This suggests that the Pb and Cu ions are prevented from taking part in the conduction possibly by the formation of metallic particles.

Evidence in support of this idea comes from the work of Bradshaw, Johnson and Shaw [4] who examined the size and distribution of Pb and Cu particles in wedge-shaped chips broken from the surface of electrolysed glass under the transmission electron microscope. Fig. 10 (a),

Table 2. Comparison of σ_x (calc) with the work of other authors

Temperature °C	Applied Voltage V	σ_x (calc) Pb/Cu anode mhos cm⁻¹	σ_x (calc) Pb anode mhos cm⁻¹	Thickness y Pb/Cu anode nm	Thickness y Pb anode nm	Conductivity I.R. silica* [2]. mhos cm⁻¹	Conductivity O.S. silica† [2]. mhos cm⁻¹	Conductivity PbOSiO₂ [3]. mhos cm⁻¹
600	25	$6\cdot8 \times 10^{-9}$		66·5		$2\cdot9 \times 10^{-8}$	1×10^{-9}	4×10^{-6}
	50	$5\cdot0 \times 10^{-8}$		280				
650	25	$1\cdot24 \times 10^{-8}$		86·0		$6\cdot7 \times 10^{-8}$	$2\cdot9 \times 10^{-9}$	1×10^{-5}
700	12		$2\cdot8 \times 10^{-8}$		210			
	25	$1\cdot41 \times 10^{-7}$	$8\cdot7 \times 10^{-8}$	284	244	1×10^{-7}	1×10^{-8}	2×10^{-5}
750	25		$1\cdot48 \times 10^{-7}$		310	$2\cdot2 \times 10^{-7}$	$2\cdot2 \times 10^{-8}$	4×10^{-5}
800	25		$4\cdot15 \times 10^{-7}$		580	$2\cdot9 \times 10^{-7}$	$4\cdot0 \times 10^{-8}$	$7\cdot1 \times 10^{-5}$

* I.R. silica Quartz crystal, electrically fused. 4 p.p.m. Na

† O.S. sillca $SiCl_4$ flame fused. 0·04 p.p.m. Na

(b) and (c) are micrographs of samples of glass treated with Pb only, with Cu only, and with Pb/Cu together. It is clear that the Pb particles are larger than the Cu particles, the most common diameters for the two materials being 56 and 16 nm respectively. From (c) it appears that in the thin part of the glass wedge, to the right of the photograph, there are only Pb particles present. By examining the glass wedge at various depths using stereo pair micrographs the authors were able to establish the distribution of the Pb and Cu in the surface layers; the results are shown in Fig. 11. The Pb and Cu particles
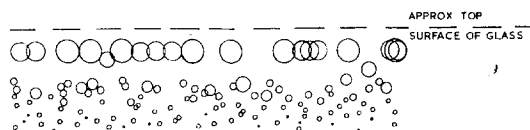

Fig. 11. Particle distribution in Pb/Cu treated surface layer.

fall into separate bands. There is first a layer of clear glass about 70 nm thick, followed by the layer of Pb particles, then a particle free gap of about 100 nm, and finally a band of the smaller particles of copper. There are about 70 of the larger and 415 of the smaller particles per square micron. Both bands of particles lie within a depth of 300 nm from the surface and this value may be compared with the thickness of the high resistance layer calculated in Table 2. The agreement is close at 700°C, the temperature at which this glass was treated.

The form of the copper has been established by electron diffraction as the crystalline metal. This conclusion is supported by the work of Fainberg [5] who reported the presence of crystalline copper X-ray patterns in lead silicate glass containing up to 10 wt % CuO which had been reduced in hydrogen at temperatures up to 480°C. Perner [6] also reached the same conclusion for copper ions replacing sodium and potassium ions in soda and potassium lime silicate glasses at temperatures up to 580°C.

While the presence of crystalline metallic copper particles is clear and unambiguous, the same cannot be said of the lead particles. Bradshaw, Johnson and Shaw [4] were unable to obtain sharp diffraction patterns for this element and Fainberg [5] was unable to find sharp X-ray diffraction patterns for his reduced lead silicate glasses containing up to 40 wt % PbO. However, Haertling and Cook [7] deduced the chemical formation of elemental lead at the surface of lead silicate glass reduced in hydrogen at 480°C from weight change measurements and dew point measurements on the reacting gases. Fainberg finally established the presence of elemental, metallic lead in his reduced glasses by DTA measurements and by increases in the initial softening temperature of reduced lead silicate glass tube due to the enrichment of the surface layers in silica. He also measured the change in the electrical conductivity of surface layers of reduced glass with time of treatment. The conductivity rose initially and then fell
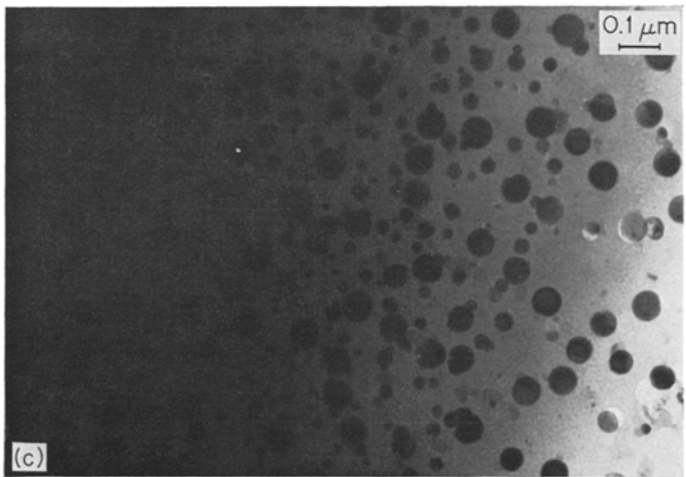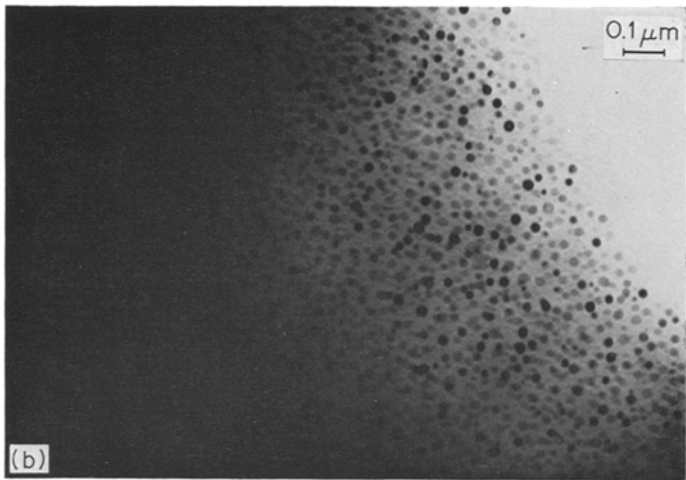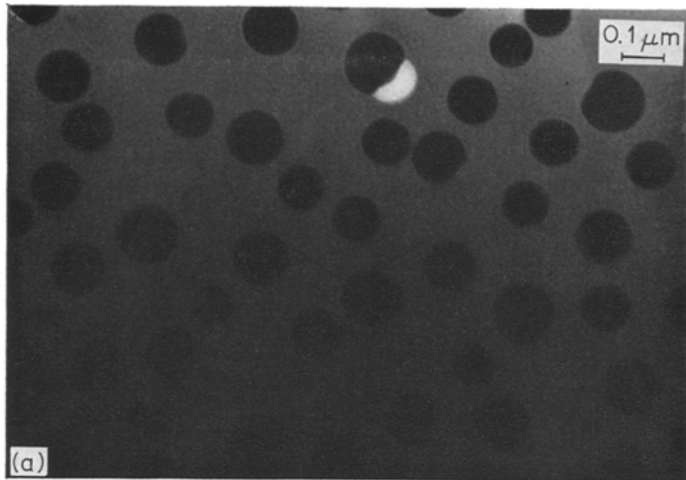
Fig. 10. Transmission electron micrographs of thin sections of electrolysed glass surface. (a) Pb treated ($\times 125\,000$). (b) Cu treated ($\times 125\,000$). (c) Pb/Cu treated ($\times 125\,000$).

and the author attributed the increase to the initial chemical formation of elemental lead and the decrease to its nucleation to lead particles. The most reasonable conclusion about the present work seems to be that the lead is present not as a compound but as elemental, metallic lead which is in the amorphous or super cooled liquid form and not as the crystalline phase.

It is assumed that the molten alloys do not diffuse into the glass before electrolysis even though the latter is softened at the higher temperatures; this is confirmed by the similarity of the I/t plots on successive pulsing.

It is also assumed that the ions are reduced to the metal by hydrogen present in the surface layers of the glass once electrolysis has taken place. The literature on hydrogen permeation and diffusion into glasses at elevated temperatures is sparse. The measurements on silica are complicated by the possibility of hydroxyl ion formation and the existence of a water-hydrogen-silica equilibrium [8–10]. However, Lee and Fry [11] give values of the diffusion constant and the solubility of deuterium in silica at 1000°C (the temperature to which the glass of Bradshaw, Johnson and Shaw was heated before electrolysis) of $1\cdot5 \times 10^{-7}$ cm^{2}s^{-1} and $1\cdot2 \times 10^{17}$ molecules cm^{-3}. Also Jorgensen and Norton [12] measured the hydrogen permeation of silica at 1000°C as 25×10^{-7} cm^{3}s^{-1} (S.T.P.) at a hydrogen pressure of 76 mm. This implies that within 20 s, hydrogen could permeate down to a depth of 500 nm. These authors also recorded a 50% increase in permeability on the application of a field of 300 V cm^{-1}. As σ_x may be 10^4 times greater than σ_{Na}, the bulk conductivity, it may be assumed that shortly after the start of electrolysis most of the 25 V applied appears across the depleted layer of, say, 500 nm thick. This will result in fields of 5×10^5 V cm^{-1} and it would be expected that under these fields any hydrogen present in the surface layer would be highly mobile resulting in reduction at the deeper levels of the layer. Copper ions should be somewhat more easily reduced than lead ions, values for the standard electrode potentials of the reactions $Cu^+ \longrightarrow Cu$ and $Pb^{++} \longrightarrow Pb$ at 700°C being 0·24 and 0·31 V, calculated from the thermodynamic data of Kubaschewski and Evans [13]. Delimarskii and Markov [14] also

give values for the decomposition potentials of the pure oxides CuO and PbO at 1000°C of 0·41 and 0·48 V, which are close. However, the copper ions may penetrate deeper into the glass before reduction than the lead ions because of their smaller size ($Cu = 0\cdot096$ nm and $Pb = 0\cdot12$ nm), and the fact that they are singly charged and the lead doubly charged.

There is some difference of opinion on the possible distribution of lead and copper ions in the surface layer between the electron microscope work and the work of Fletcher and Tune [15] and Cundall and Leach [16]. Fletcher and Tune etched the surface layers of electrolysed glass with 1% HF etchant in steps of 10 nm and measured the Cu and Pb concentrations with atomic absorption spectroscopy and polarography, respectively. They found that the Pb concentration increased with depth of penetration but that the highest copper concentration occurred at the surface and to a depth of 40 nm. Chemical analysis will detect copper in both the metallic and ionic form and, of course, the latter would not be seen on the electron micrographs. This is the probable explanation of the discrepancy between the two sets of results.

Cundall and Leach used electron spectroscopy (ESCA) to follow the element distribution in the surface layers of treated glass etched to various depths by argon ion etching. They also found that the copper concentration was highest at the surface and that the lead concentration increased to a maximum at 50 nm and then fell. As the photoelectrons emitted on X-ray irradiation originate from between 1 to 10 nm below the specimen surface, the technique is a sensitive one and again detects the elements in both the ionic and metallic states.

While there is some disagreement between the various sets of results it does seem clear from the electron micrographs that metallic lead and copper particles do exist in considerable concentration in a surface layer of about 300 nm. The presence of this non-ionic material would explain the low conductivity of the treated layer which is observed and the assumption on which the mathematical treatment of the $1/I^2$ against t kinetics is based, viz., the existence near the surface of a high resistance layer, would seem to be justified.

Acknowledgements

Appendix

Derivation of an expression for the variation of current density with time during the electrolysis (after J. A. Yates, unpublished work).

It is assumed that during the electrolysis the interstitial sodium ions are replaced by another cation x and that this gives rise to a surface layer of specific conductivity σ_x which is different from the specific conductivity of the base glass σ_{Na}.

Then, if Ohm's law applies:

$$I = \sigma_x \frac{V_x}{y} \qquad (1)$$

where I is the current density and V_x the voltage drop across a layer of thickness y and specific conductivity σ_x.

Also, considering the base glass:

$$I = \sigma_{Na} \cdot \frac{V - V_x}{l - y} \approx \sigma_{Na} \frac{V - V_x}{l} \qquad (2)$$

since l, the thickness of the sample, is much greater than the surface layer thickness.

It is assumed that the rate of penetration is proportional to the current, or:

$$\frac{dy}{dt} = \frac{I}{Fc} \qquad (3)$$

where F is Faraday's constant and c is the con-

centration of replaceable ions in equivalents per millilitre.

Eliminating V_x from (1) and (2):

$$y = \frac{\sigma_x}{I}\left[V - \frac{Il}{\sigma_{Na}} \right] \qquad (4)$$

Differentiating:

$$\frac{dy}{dt} = - \frac{\sigma_x \cdot V}{I^2} \cdot \frac{dI}{dt} \qquad (5)$$

Substituting from Equation (3):

$$\frac{I}{Fc} = - \frac{\sigma_x \cdot V}{I^2} \cdot \frac{dI}{dt} \qquad (6)$$

Integrating:

$$t = \left[\frac{\sigma_x \cdot V Fc}{2 I^2} \right]_{I_0}^{I} \qquad (7)$$

where I_0 is the current at $t = 0$ i.e.:

$$I_0 = \frac{\sigma_{Na} V}{l} \qquad (8)$$

Substituting the limits:

$$t = \frac{\sigma_x V Fc}{2}\left(\frac{1}{I^2} - \frac{l^2}{\sigma_{Na}^2 V^2} \right) \qquad (9)$$

Rearranging this gives:

$$I = \left[\frac{\frac{1}{2} V \sigma_x Fc}{t + \dfrac{\sigma_x Fc\, l^2}{2\, \sigma_{Na}^2 V}} \right]^{\frac{1}{2}} \qquad (10)$$

References

[1] J. K. Higgins, *J. Appl. Electrochem.*, **2** (1972) 1.
[2] A. E. Owen and R. W. Douglas, *Journ. Soc. Glass Tech.*, **43** (1959) 159 T.
[3] S. W. Strauss, D. G. Moore, W. N. Harrison and L. E. Richards, *J. Res. Natl. Bur. of Standards*, **56** (1956) 135.
[4] J. M. Bradshaw, K. A. Johnson and B. W. Shaw, SC/72/124. (Internal R. & D. Report Lathom.)
[5] A. E. Fainberg, *Zhur. Priklad. Khim.*, **38** (1965) 2192, *Izvestiya. Akad. Nauk SSSR, Neorganich. Mat.*, **2** (1966) 1154.
[6] B. Perner, *Silikaty*, **7** (1963) 109.
[7] G. H. Haertling and R. L. Cook, *J. Amer. Ceram. Soc.*, **48** (1965) 35.
[8] G. Hetherington and K. M. Jack, *Phys. Chem. of Glasses*, **3** (1962) 129.
[9] T. Bell, G. Hetherington and K. M. Jack, *Phys. Chem. of Glasses*, **3** (1962) 141.
[10] V. Garino Canina and M. Priqueler, *Phys. Chem. of Glasses*, **3** (1962) 43.

[11] R. W. Lee and D. L. Fry, *Phys. Chem. of Glasses*, **7** (1966) 19.

[12] P. J. Jorgensen and F. J. Norton, *Phys. Chem. of Glasses*, **10** (1969) 23.

[13] O. Kubaschewski and E. Evans, *Metallurgical Thermochemistry*, p. 336, Pergamon Press, London (1958).

[14] Y. K. Delimarskii and B. F. Markov, *Electrochemistry of Fused Salts*, p. 148, The Sigma Press New York (1961).

[15] E. Fletcher and A. Tune, SC/72/34. (Internal R. & D. Report, Lathom.)

[16] J. A. Cundall and R. J. Leech, SC/72/36. (Internal R. & D. Report, Lathom.)